ADVANCED FUNCTIONAL MATERIALS
www.afm-journal.de

www.MaterialsViews.com

A Review of Surface Plasmon Resonance-Enhanced Photocatalysis

*Wenbo Hou and Stephen B. Cronin**

In the past decade, the surface plasmon resonance of Ag and Au nanoparticles has been investigated to improve the efficiency of photocatalytic processes. The photocatalytic production of fuels is particularly interesting for its ability to store the sun's energy in chemical bonds that can be released later without producing harmful byproducts. This Feature Article reviews recent work demonstrating plasmon-enhanced photocatalytic water splitting, reduction of CO_2 with H_2O to form hydrocarbon fuels, and degradation of organic molecules. Focus is placed on several possible mechanisms that have been previously discussed in the literature. A particular emphasis is given to several aspects of these mechanisms that are not fully understood and will require further investigation.

1. Introduction

In photocatalytic processes, the energy of photons can be used to drive many useful chemical reactions, including solar production of fuels and water purification. While these photocatalytic processes are potential very useful, their efficiency is far too low for practical large scale applications. Direct solar to chemical energy conversion, however, has several advantages over solar-to-electric energy conversion. For example, as an intermittent light source, there is no way of storing large amounts (≈GW) of electricity to be used during the night. The photocatalytic production of fuels provides an alternative method for storing the sun's energy in chemical bonds that can be released later without producing harmful byproducts. Over the past several years, a new method for improving the efficiency of photocatalytic processes has emerged, involving the strong plasmon resonance of Ag and Au nanoparticles. In this Feature Article, we focus on recent work demonstrating plasmon-enhanced photocatalytic water splitting, reduction of CO_2 with H_2O to form hydrocarbon fuels, and degradation of organic molecules. While the idea of coupling strongly plasmonic nanoparticles to photocatalytically active supports may seem straightforward, there are several subtleties required in order to achieve a net enhancement in photocatalysis. These will be discussed in light of several possible mechanisms that have been previously discussed in the literature.

Dr. W. Hou
Departments of Chemistry
University of Southern California
Los Angeles, CA 90089, USA
Prof. S. B. Cronin
Departments of Chemistry
Physics, and Electrical Engineering
University of Southern California
Los Angeles, CA 90089, USA
E-mail: scronin@usc.edu

DOI: 10.1002/adfm.201202148

2. Metal Oxide Catalysts

Metal oxides (e.g., TiO_2, Fe_2O_3, PbO) are promising photocatalysts for a number of applications, including solar fuel production, oxidation of pollutants, and anti-fogging/self-cleaning coatings for windows and lenses. As a self-cleaning catalyst, TiO_2 does not suffer from the corrosion problems associated with photovoltaic cells. Fujishima and Honda first demonstrated the photochemical splitting of water on *n*-type TiO_2 electrodes using UV light.[1] The absorption of light is necessary to initiate the charge transfer mechanism of the catalytic process, as shown below in **Figure 1**a. In TiO_2, an absorbed photon creates an electron-hole pair. The electrons drive a reduction of the H^+ ions to produce H_2 gas, while the holes drive the oxidation of the OH^- ions, producing O_2 gas. While TiO_2 is one of the most promising photocatalysts, it does not absorb light in the visible region of the electromagnetic spectrum. Figure 1b shows this problem graphically with the absorption spectrum of TiO_2 superimposed over the solar spectrum (AM 1.5).[2] Because of TiO_2's short wavelength cutoff, there are very few solar photons (≈4%) that can be used to drive this photocatalyst. Several attempts to extend the cutoff wavelength of this material by doping have resulted in significantly improved efficiencies in the visible range.[3–5] Hematite (α-Fe_2O_3) is another well-known photocatalyst for water splitting and methane production.[6–9] With a smaller band gap (2–2.3 eV), Fe_2O_3 can capture approximately 40% of the incident sunlight, also illustrated in Figure 1b. While Fe_2O_3 is highly stable over a wide range of pH environments, it typically requires the application of an external bias to initiate the hydrogen evolution reaction, as discussed below.[10]

Figure 1c shows the approximate flat band positions of several metal oxide semiconductors together with the redox potentials of the water splitting half-reactions at pH = 7 with respect to NHE (normal hydrogen electrode).[11] TiO_2 is an excellent photocatalyst for two main reasons. The first is the relative positions of its conduction and valence bands with respect to the reduction and oxidation potentials of H_2O. While the conduction and valence bands of TiO_2 do not quite straddle both the reduction and oxidation potentials of H_2O, photocatalytic water

splitting is made possible by adjusting the pH of the solution and/or doping the TiO_2. That is, by making the TiO_2 conduction band higher than the H_2/H_2O potential, spontaneous transfer of electrons will occur from the titania conduction band to the H_2O molecules in solution, driving the reduction half reaction forward. Similarly, since the TiO_2 valence band lies well below the H_2O/O_2 potential, spontaneous transfer of holes occurs from the valence band to the H_2O molecules, driving the oxidation half reaction forward. The second reason is that titania is oxidatively stable, even with slight defects, over a wide range of oxidative and reductive environments.

3. Surface Plasmon Resonance

Plasmons are the collective oscillation of the free charge in a conducting material. Light below the plasma frequency is reflected because the electrons in the metal screen the electric field of the light. Light above the plasma frequency is transmitted because the electrons cannot respond fast enough to screen it. Surface plasmons are oscillations confined to the surfaces of conducting materials and interact strongly with light. A resonance in the absorption occurs at the plasmon frequency when the real part of the dielectric function goes to zero. Irradiating metal nanoparticles with light at their plasmon frequency generates intense electric fields at the surface of the nanoparticles. The frequency of this resonance can be tuned by varying the nanoparticle size, shape, material, and proximity to other nanoparticles.[12–15] For example, the plasmon resonance of silver, which lies in the UV, can be shifted into the visible range by making the nanoparticle size very small. Similarly, it is possible to shift the plasmon resonance of gold from the visible range into the infrared wavelength range by minimizing the nanoparticle size. Nurmikko and others have fabricated arrays of nanoparticles with different spacing using electron beam lithography.[12,16] This was corroborated by the calculations of Zou et al. using an interacting dipole model for calculating the plasmon resonance of two nearly touching nanoparticles.[17] The intense electric fields produced near plasmon resonant metallic nanoparticles are currently utilized in surface enhanced Raman spectroscopy (SERS) to produce enhancement factors as high as 10^{14}.[18–20] Numerical simulations have predicted SERS enhancement factors up to 10^{10}.[21,22]

4. Photocatalytic Processes

4.1. Photocatalytic Decomposition of Organic Compounds

A vast majority of the publications in the literature discussing plasmon-enhanced photocatalysis have focused on reactions involving photocatalytic decomposition of organic compounds.[23–54] These are typically dye molecules (e.g., methyl orange) whose decomposition rates can be easily observed by optical means.[44] In photocatalytic degradation, photogenerated electrons reduce adsorbed oxygen (O_2) to form superoxide ($HO_2\cdot$) radicals and photogenerated holes react with H_2O to form $OH\cdot$ radicals.[55] Hydroxyl radicals subsequently oxidize the organic pollutants resulting in mineralization and complete degradation.[55–57] These pollutants are broken down into small molecules such as CO_2, H_2O, and NH_3, which are not particularly toxic. While most scientific works study the decomposition of dye molecules, this basic process is applicable to industrial pollutants, such as perchloroethane, pesticides, and pharmaceutical drugs. Enhanced photodegradation of organic compounds has been observed after adding Au or Ag nanoparticles to several semiconductor photocatalysts including, TiO_2,[23,24,28,30,34,35,37–39,41,44,45,47,49,53,54,58] ZrO_2,[42] ZnO,[28] Cu_2O,[50] SnO_2,[36] CeO_2,[42] Fe_2O_3,[42] SiO_2,[42,52] $KNbO_3$[32] under both UV[23–41] and visible illumination.[31,32,35,38,42–54] In a number of these studies, semiconductor nanoparticles are synthesized by the sol gel method, while gold nanoparticles are introduced following the general recipe of reducing a gold salt.[59]

4.2. Photocatalytic Water Splitting

By depositing plasmonic metal nanoparticles on top of anatase TiO_2, several research groups have observed enhanced photocatalytic water splitting under visible illumination.[60–64] In this reaction, photocurrents were measured using a potentiostat, and the H_2 formed was monitored using gas chromotography

Stephen B. Cronin received his Ph.D. in physics from the Massachusetts Institute of Technology in 2002 with advisor Prof. Mildred Dresselhaus. He received his post-doctoral training in the Department of Physics at Harvard University (2002–2005) working under Prof. Michael Tinkham. He is presently an Associate Professor and Gordon S. Marshall Early Career Chair in Engineering at the University of Southern California in the departments of electrical engineering, chemistry, and physics.

Wenbo Hou received her Ph.D. from Prof. Stephen B. Cronin's research group in the Department of Chemistry at the University of Southern California in 2012. She received her Bachelor degree in Chemistry from the Beijing Normal University and Master degree in Chemistry from the University of Saskatchewan. She currently works as a postdoctoral research fellow at Lawrence Berkeley National Laboratory.

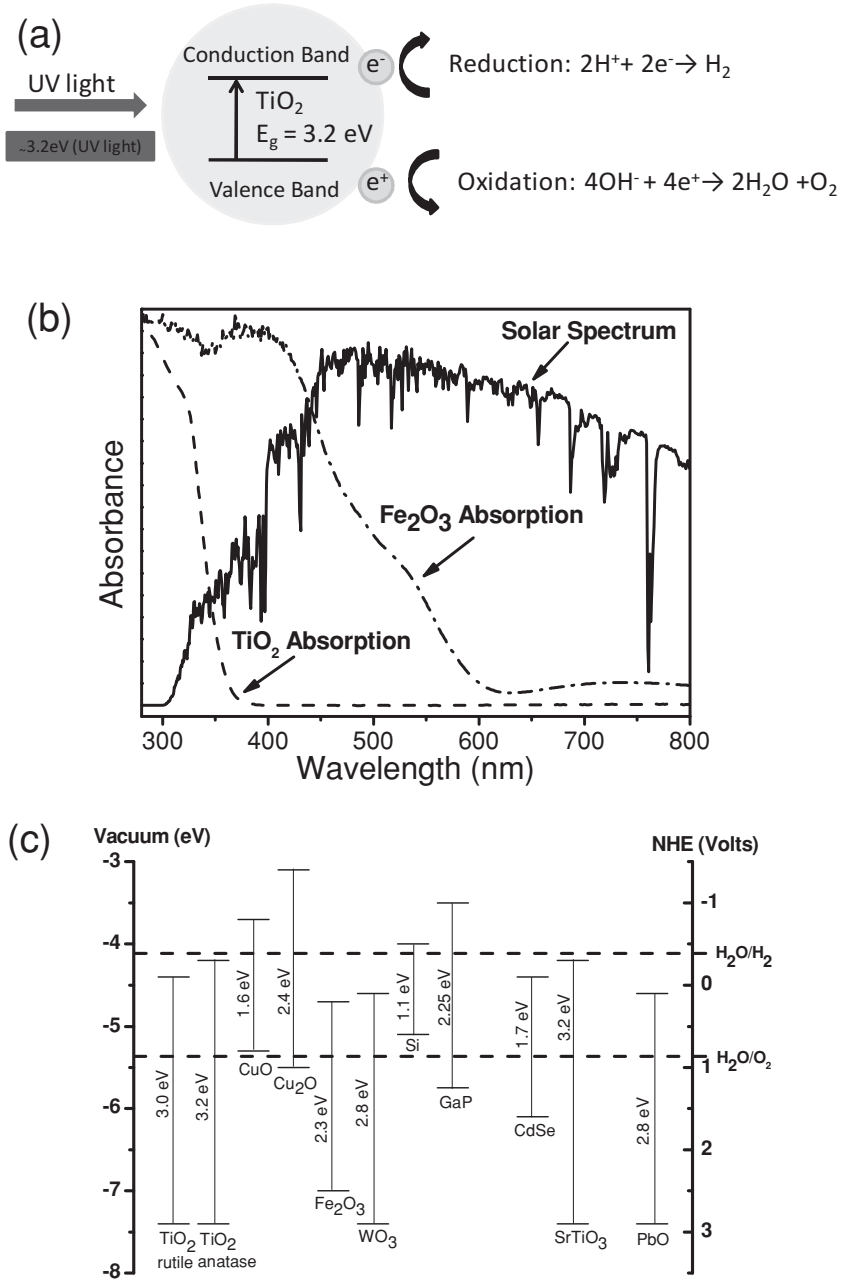

Figure 1. a) Schematic diagram illustrating the photochemical oxidation and reduction processes of TiO_2. b) Solar spectrum and absorption spectra of TiO_2 and Fe_2O_3. c) Energy band diagram of various metal oxide semiconductors, together with the redox potentials of water splitting.

and/or mass spectrometry. Liu et al. observed enhanced photocurrents in the water splitting reaction under visible illumination by depositing Au nanoparticles on top of anodic TiO_2, with enhancement factors of 5 and 66 at 532 nm and 633 nm, respectively.[61] Duan et al. also reported similar enhancement for Ag nanoparticles on CdS with a particular emphasis on the SiO_2 intermediate layer between CdS and Ag, which plays an important role in tuning the plasmon resonance peak.[60] Torimoto et al. also demonstrated enhanced photocatalytic activity for photocatalytic water splitting by deposition of CdS on Au@SiO_2 particles.[64] Ingram et al. observed a 10-fold enhancement in the visible-light photocurrent of water splitting catalyzed by Ag/N-TiO_2 compared with that catalyzed by bare N-TiO_2. They also found that the photocurrent follows first- and half-order intensity dependences in the Ag/N-TiO_2 and N-TiO_2, respectively, as shown in **Figure 2**a. The observed linear dependence of the photocurrent on the light intensity for Ag/N-TiO_2 shows that charge carriers are formed close to the semiconductor surface in the composite Ag/N-TiO_2 system.[65] Thomann et al. measured the photocurrent enhancement spectrum of Au/Fe_2O_3-photocatalyzed water splitting with a peak enhancement of approximately 11×, as shown in Figure 2b. They also found that the peak position and the line shape of the photocurrent enhancement depend critically on the position of the nanoparticles in the iron oxide film. Particles on top of the absorber film produce an asymmetric line shape of the photocurrent enhancement, while particles embedded in produce a more symmetric spectral feature.[10] Several studies have focused on establishing the optimum Au wt% in TiO_2 rather than nanoparticle geometry.[62,63] However, the optimum Au wt% will depend strongly on the particular morphology of the photocatalytic semiconductor (e.g., mesoporous, nanoparticle, thin film), and does not lend any significant insight into the underlying physical mechanism of enhancement. While the plasmonic enhancement factors reported above are relatively large, the overall photoconversion efficiencies are still quite low particularly in the visible wavelength range. The photoconversion efficiency for water splitting is reported to be around 1% under an overpotential of 0.6 V.[3] No one has reported an actual value for the photoconversion efficiency of organic molecule decomposition.

4.3. Photocatalytic Methane Formation

Plasmonic enhancement has also been demonstrated in photocatalytic methane formation by the reduction of CO_2 with H_2O: $CO_2 + 2H_2O \rightarrow CH_4 + 2O_2$.[66] Prior to plasmon-enhanced studies, photocatalytic methane formation has been studied by Grime's group[67–69] and several others.[70–74] The products formed have been identified qualitatively and quantitatively by gas chromatography as shown in **Figure 3**a. This reaction is more complicated process than water splitting reaction, involving eight photons to reduce CO_2 into CH_4. In addition to methane, methanol, formaldehyde are also possible products. In Figure 3b, the energy band

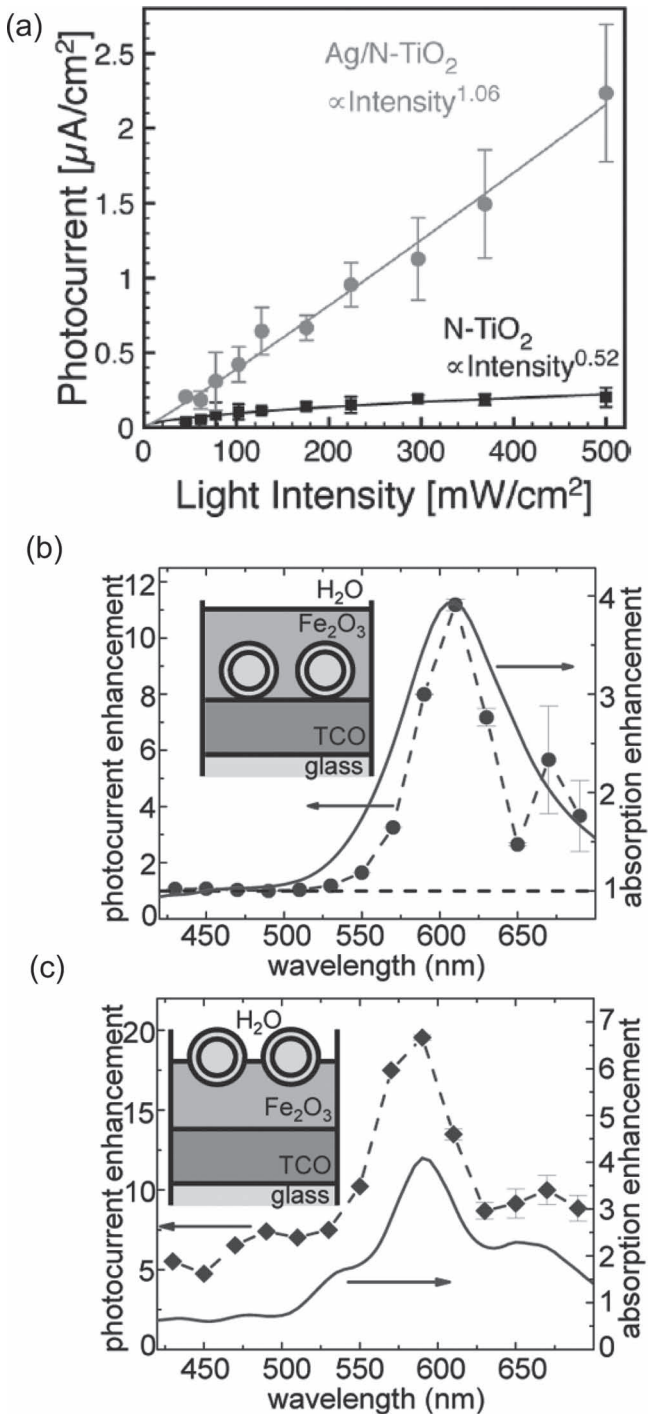

Figure 2. a) Photocurrent plotted as a function of broadband visiblelight intensity for N-TiO_2 and composite Ag/N-TiO_2 samples. The Ag/N-TiO_2 exhibits approximately a linear (first-order) dependence on the light intensity, while the N-TiO_2 exhibits an approximately halforder dependence. Reproduced with permission.[65] Copyright 2011, American Chemical Society. Photocurrent enhancement spectra for Au nanoparticles with a silica shell b) embedded in and c) on top of a 100-nm thin Fe_2O_3 photoelectrode layer. Measured photocurrent and simulated absorption spectra are shown by red symbols and solid blue lines, respectively. Reproduced with permission.[10] Copyright 2011, American Chemical Society.

diagram shows the conduction band and valence bands of TiO_2 together with the reduction potentials for several possible products: CH_4, HCHO, and CH_3OH. The conduction band edge and photovoltage of TiO_2 are just barely high enough to carry out direct CO_2 reduction and water oxidation. Because of this, an additional CO_2 reduction catalyst is typically needed in order to accomplish reasonable CO_2 reduction directly on a semiconductor surface. Other products can also become energetically favorable in the presence of co-catalysts and under different pressures, which change the electron energies and the reduction potentials for each product.[66,70,71,75–78] Future studies are needed in order to separate the effects of barrier reduction co-catalysts and plasmonic enhancement. Photocatalytic CO_2 reduction is a more challenging problem than solar water splitting due to its requirement of conduction band edge, additional photovoltage, and multielectron processes. A detailed mechanism of pyridinium-catalyzed CO_2 reduction through several sequential electron transfers instead of a multielectron transfer has been given by Bocarsly's group.[79] In the case of plasmon-enhanced photocatalysis, further investigation is needed in order to establish these reaction pathways. Recently, Hou et al. found the quantum efficiency to be improved by a factor of 24 under visible illumination by integrating Au nanoparticles with TiO_2 (2.1×10^{-5}% for Au/TiO_2 and 8.8×10^{-7}% for bare TiO_2).[66]

In the photocatalytic reduction of CO_2 with H_2O, $^{13}CO_2$ isotopes have been used to identify the origin of CO intermediate products using diffuse reflectance infrared Fourier transform (DRIFT) spectroscopy.[80] While a ^{13}CO peak was observed, ^{12}CO was found to be the primary product, indicating that carbon residues on the catalyst surface are involved in the reaction. Later, Yui et al. measured TiO_2 treated to remove organic adsorbates, also using isotopically labeled $^{13}CO_2$. For bare TiO_2, CO was photocatalytically generated as the main product, originating from the CO_2 feedstock rather than from surface residue.[81] By depositing Pd (>0.5 wt%) on the TiO_2 (void of organic adsorbates), however, CH_4 was observed as the main product, indicating that the metal-semiconductor interface plays an important role in the reaction pathway and products. Since TiO_2 is a strong oxidant and is known to oxidize organic impurities, ^{13}C isotopologues should be used in future studies in order to verify the origin of any carbonaceous species produced in these catalytic processes.

5. Discussion of Photocatalytic Enhancement Mechanisms

Two main mechanisms have been discussed in the literature regarding plasmonic enhancement of photocatalysis under visible illumination: charge transfer and local electric field enhancement. We discuss these possible mechanisms in more detail below.

5.1. Charge Transfer Mechanism

In 2004, Tatsuma's group proposed a charge transfer mechanism to explain their experimentally observed photon-to-current

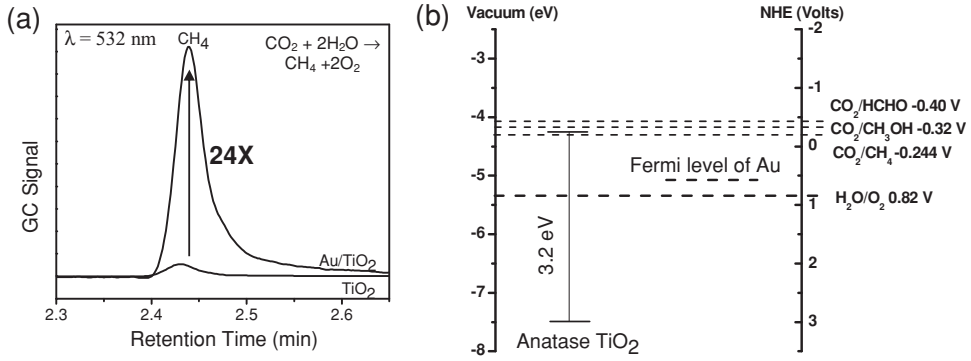

Figure 3. a) Methane signals measured by gas chromatography for bare TiO_2- and Au/TiO_2-catalyzed CO_2 reduction. b) Energy band alignment of anatase TiO_2, Au and the relevant redox potentials for several possible products. Reproduced with permission.[66] Copyright 2011, American Chemical Society.

conversion efficiency (IPCE) enhancement under visible light illumination upon loading Au or Ag nanoparticles into TiO_2 sol gel films.[82–84] In their proposed charge transfer mechanism, the plasmon resonance excites electrons in Au or Ag, which are then transferred to the conduction band of the adjacent TiO_2, as shown schematically in **Figure 4**. This charge transfer mechanism is similar to that of a dye-sensitized solar cell.[85] Subsequently, several other groups used this mechanism to explain enhanced photocatalytic water splitting,[63] methyl orange decomposition,[38] and photo-oxidation of formaldehyde[86] observed under visible illumination. While this charge transfer mechanism has been cited by many groups, surface plasmons consist of a charge density wave on the surface of the metal, and therefore have no HOMO-LUMO or analogous valence band-conduction band energy separation associated with them. All the plasmonic charge resides at the Fermi energy of the metal, and, therefore, is not able to drive the reduction and oxidation half-reactions, as described above for metal oxide semiconductors. That is, the plasmonic electrons (at E_F) are too low in energy to drive the reduction half-reaction, and the plasmonic holes (also at E_F) are too high in energy to drive the oxidation half-reaction. The visible light photoactivity of few atom-metal clusters has been shown in a several recent studies.[87–89] For example, Ag_8 and Au_{25} clusters exhibit molecular-like excited-state properties with well-defined absorption and emission features. Therefore, these metal nanoclusters are photochemically reactive, and act as electron-donors due to their molecule-like properties.[87–89] The size of the nanoparticles used in the plasmonic studies are typically one order of magnitude larger than these clusters, and behave electronically like bulk Au and Ag. Furthermore, when the size of metal nanoparticles is reduced to around 2 nm or less, their optical absorption cross section becomes very small and plasmonic effects become negligible.[89–91] At these small size scales, the localized surface plasmon resonance disappears, as the band structure becomes discontinuous and broken down into discrete energy levels.

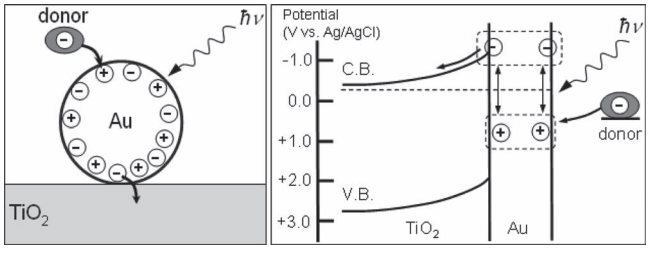

Figure 4. Schematic illustration of the proposed charge transfer mechanism. Reproduced with permission.[84] Copyright 2005, American Chemical Society.

Using femtosecond transient absorption spectroscopy with an IR probe, Furube et al. showed evidence of plasmon-induced electron transfer from 10-nm gold nanodots to TiO_2 nanoparticles.[92] In 2011, Moskovits et al. further explained this charge transfer mechanism, in which the surface plasmon decay produces electron-hole pairs in the gold. The resulting hot electrons are then directly injected into TiO_2 by quantum tunneling.[93] It should be noted, however, that these carrier dynamics studies did not involve redox reactions, and therefore were not limited by the Fermi energy of the metal, which lies below the potential of the reduction half-reaction. Halas' group reported an active optical antenna device that uses the hot electron-hole pairs arising from plasmon decay to directly generate a photocurrent, resulting in the detection of light.[94] Since this study also did not involve redox reactions, the photocurrent generation is not limited by the difference between the Fermi energy of the metal and the potential of the reduction half-reaction.

5.2. Local Electric Field Enhancement

As mentioned above, irradiating metal nanoparticles near their plasmon resonance frequency can generate intense local electric fields near the surface of the nanoparticles. Electromagnetic simulations using the finite-difference time-domain (FDTD) method have shown that the electric field intensity of local plasmonic "hot spots" can reach as much as 1000 times that of the incident electric field.[95,96] In these "hot spot" regions, the electron-hole pair generation rate is 1000 times that of the incident electromagnetic field. Thus, an increased amount of photo-induced charge is generated locally in the TiO_2 due to the local field enhancement of the plasmonic nanoparticles. This enhancement mechanism also relies on the presence of defect states in the TiO_2, which are needed in order to enable light absorption below the band gap of the semiconductor, as

discussed below. Mizeikis et al. performed simulations of optical field enhancement in a system consisting of spherical and hemispherical noble metal nanoparticles on a smooth titania surface using the FDTD method.[97] Large near-field enhancement factors up to 10^4 were obtained at the metal/titania interface in their simulations.[97] Cronin's group has attributed photocatalytic enhancement to this plasmonic local electric field enhancement.[44,61,66] Several other groups have also adopted the local electric field enhancement mechanism.[45,49,60,64,98–100] Lu et al. ascribed a 2.3-fold increase in 2,4-dichlorophenol degradation catalyzed by Au nanoparticle/TiO_2 to the enhanced light harvesting caused by the surface plasmon resonance.[49] Linic's group also attributed their observed photocatalytic improvement to the enhancement in the intensity of electric fields compared with the field intensity of the incoming photon flux.[45,98] Duan et al. investigated enhanced electron-hole pair generation rates in CdS by the enhanced near-field amplitudes of the surface plasmon resonance on the Ag surface in a Ag/SiO_2/CdS multilayer nanocomposite. They demonstrated that the thickness ratio of the Ag, SiO_2, and CdS layers plays an important role in the near-field enhancement.[60] Torimoto et al. also indicated that the surface plasmon resonance-induced electric field and photocatalytic activity of Au/SiO_2/CdS for photocatalytic water splitting greatly depend on the distance between CdS and Au nanoparticles, in further support of this near-field electromagnetic enhancement mechanism.[64]

Kamat et al. and Takai et al. have reported that metal nanoparticles can also act as a reservoir for photogenerated electrons in semiconductors.[40,101–104] Here, photoexcited electrons in the semiconductor transfer from the conduction band to the metal nanoparticles. The storage of electrons, observed through a blue-shift in the surface plasmon frequency, undergoes charge equilibration with a photoexcited semiconductor and drives the Fermi level to more negative potentials.[105–107] This storage of electrons in metal nanoparticles reduces charge recombination, thereby enhancing the photocatalytic activity. This electron storage mechanism can play a significant role in the photocatalytic enhancement under UV illumination, since UV light has enough energy to drive the electron-hole pair generation in TiO_2. In addition to strongly plasmonic Au and Ag-modified photocatalysts, this enhancement mechanism has been observed in other metals, including Pt.[105–107]

5.3. Light Absorption/Carrier Diffusion Length Problem

One important problem in photocatalysts is the inherent mismatch between the light absorption length and the minority carrier diffusion length. **Figure 5**a illustrates this problem schematically for *n*-type TiO_2, where a relatively thick film is needed to absorb a majority of the incident light at $\lambda = 550$ nm.[108] However, the minority carriers (holes) recombine rapidly with the majority carriers (electrons) over a much shorter length scale. Because of the extremely short minority carrier diffusion length, most of the photo-generated carriers recombine before reaching the semiconductor-electrolyte interface and, therefore, do not contribute to the photocatalysis.[108,109] Localized plasmonic fields provide a way to mitigate this problem by coupling light very effectively from the far-field to the near-field at the metal oxide/electrolyte interface, as illustrated in Figure 5b. As a result, most of the photogenerated charge will diffuse to the surface and contribute to catalysis. For this reason, this local electric field enhancement produces a net enhancement in the overall photocatalytic yield, despite the inherent loss in surface area of the semiconductor photocatalyst.

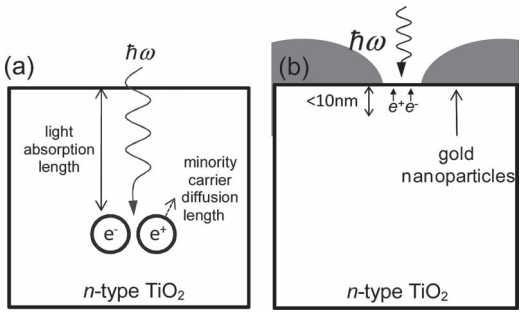

Figure 5. a) Diagram illustrating the light absorption length/minority carrier diffusion length mismatch in TiO_2. b) Diagram illustrating the local field enhancement of gold nanoparticles.

5.4. Electromagnetic Simulations

In order to understand the underlying mechanism of catalytic enhancement, Thomann et al. simulated electric field distributions generated by bare Au nanoparticles on top of iron oxide which explain the asymmetric line shape versus wavelength in photocurrent enhancement spectrum.[10] Linic's group showed the FDTD-calculated field enhancements around a 120-nm Ag cube in water as a function of the distance d from the cube.[65] Liu et al. have calculated the photocatalytic enhancement factor (EF) based on the results of FDTD simulations. Since the photon absorption rate is proportional to the electric field squared ($|E|^2$), we integrate $|E|^2$ over the whole film and divide by the integral of the incident electromagnetic field squared ($|E_o|^2$), as shown in the following equation. In the *z*-dimension, we integrate only from the TiO_2 surface ($z = 0$) to one minority carrier diffusion length below the surface ($z = -10$ nm). The value for the EF when integrating over the whole simulation area (400 nm × 300 nm) is 12, which is consistent with the values observed experimentally.[44,61]

$$\mathrm{EF} = \frac{\int_{-10\,\mathrm{nm}}^{0} dz \int dx dy |E|^2}{\int_{-10\,\mathrm{nm}}^{0} dz \int dx dy |\mathrm{E_o}|^2}$$

5.5. Doping

Since the plasmon resonance of metal nanoparticles lies lower in energy than the bandgap of most photocatalytic metal oxide semiconductors (e.g., TiO_2), doping plays an important role in this electric field enhancement mechanism and plasmon-enhanced photocatalysis. In particular, defect states are needed in order to enable light absorption below the bandgap of the semiconductor. In order for efficiency energy and charge transfer to take place between the metal nanoparticles and

the semiconductor photocatalyst, it is important that the spectral enhancement of the metal nanoparticles overlap with the spectral absorption of the semiconductor photocatalyst, and of course with the spectrum of the illumination source (i.e., the solar spectrum). This is a crucial factor for reaching maximum plasmon enhancement. Ingram et al. showed that Ag cube-modified TiO_2 has higher photocatalytic activity for methylene blue photolysis than Au sphere-modified TiO_2 because the surface plasmon resonance of Ag cubes overlaps with the solar spectrum better than that of Au spheres. They also showed that the overlap of the semiconductor absorption spectrum and the solar spectrum is also important. N-doped TiO_2 works better than undoped TiO_2 due to defect states created by N-doping, which enable sub-bandgap absorption.[45] Anodic TiO_2 (ATO) is known to have a significant amount of defects and impurities that introduced during the anodization process, which also enable sub-bandgap absorption.[44,61]

6. Conclusions

Plasmonic enhancement has been reported consistently by many research groups in several photochemical processes, including water splitting, methane formation/CO_2 reduction, and decomposition of organic molecules. The mechanism(s) underlying this enhancement, however, remain inconsistent within the field. In this Feature Article, we have summarized several possible mechanisms that have been put forth previously in the literature, namely charge transfer and local electric field enhancement. Other important aspects of these mechanisms have also been discussed, including defects and doping, the Fermi energy of the metal, and the light absorption/carrier diffusion length problem, all of which have important implications on these photocatalytic enhancement mechanisms. Surface plasmon resonant enhancement of photocatalysis is a complex multifaceted process, which requires the consideration of many material parameters including doping, bandgap, plasmonic nanoparticles/photocatalytic semiconductor morphology. While most of these aspects have been studied in some detail, it is difficult to compare the results of different studies because of the wide range in materials preparation and properties. Further studies are needed in order to fully understand these effects and to optimize this phenomenon for maximum photoconversion efficiency.

Acknowledgements

This research was supported in part by ONR Award No. N00014-12-1-0570 (W.H.) and NSF Award No. CBET-0846725 (S.C.).

Received: July 30, 2012
Revised: October 5, 2012
Published online: October 30, 2012

[1] A. Fujishima, K. Honda, *Nature* **1972**, *238*, 37–38.
[2] J. H. Seinfeld, S. N. Pandis, *Atmospheric Chemistry and Physics*, Wiley, New York **1998**.
[3] S. U. M. Khan, M. Al-Shahry, W. B. Ingler, *Science* **2002**, *297*, 2243–2245.
[4] W. Y. Choi, A. Termin, M. R. Hoffmann, *J. Phys. Chem.* **1994**, *98*, 13669–13679.
[5] M. Anpo, *Pure Appl. Chem.* **2000**, *72*, 1787–1792.
[6] J. K. Leland, A. J. Bard, *J. Phys. Chem.* **1987**, *91*, 5076–5083.
[7] R. Shinar, J. H. Kennedy, *Sol. Energy Mater.* **1982**, *6*, 323–335.
[8] M. M. Khader, G. H. Vurens, I. K. Kim, M. Salmeron, G. A. Somorjai, *J. Am. Chem. Soc.* **1987**, *109*, 3581–3585.
[9] A. Kay, I. Cesar, M. Gratzel, *J. Am. Chem. Soc.* **2006**, *128*, 15714–15721.
[10] I. Thomann, B. A. Pinaud, Z. B. Chen, B. M. Clemens, T. F. Jaramillo, M. L. Brongersma, *Nano Lett.* **2011**, *11*, 3440–3446.
[11] N. Serpone, E. Pelizzetti, *Photocatalysis,* Wiley, New York **1989**.
[12] T. Atay, J. H. Song, A. V. Nurmikko, *Nano Lett.* **2004**, *4*, 1627–1631.
[13] K. H. Kim, A. Husakou, J. Herrmann, *Opt. Express* **2010**, *18*, 7488–7496.
[14] K. Kolwas, A. Derkachova, M. Shopa, *J. Quant. Spectrosc. Radiat. Transfer* **2009**, *110*, 1490–1501.
[15] J. J. Mock, M. Barbic, D. R. Smith, D. A. Schultz, S. Schultz, *J. Chem. Phys.* **2002**, *116*, 6755–6759.
[16] K. H. Su, Q. H. Wei, X. Zhang, J. J. Mock, D. R. Smith, S. Schultz, *Nano Lett.* **2003**, *3*, 1087–1090.
[17] S. L. Zou, G. C. Schatz, *Chem. Phys. Lett.* **2005**, *403*, 62–67.
[18] K. Kneipp, Y. Wang, H. Kneipp, L. T. Perelman, I. Itzkan, R. Dasari, M. S. Feld, *Phys. Rev. Lett.* **1997**, *78*, 1667–1670.
[19] K. Kneipp, H. Kneipp, P. Corio, S. D. M. Brown, K. Shafer, J. Motz, L. T. Perelman, E. B. Hanlon, A. Marucci, G. Dresselhaus, M. S. Dresselhaus, *Phys. Rev. Lett.* **2000**, *84*, 3470–3473.
[20] R. Kumar, H. Zhou, S. B. Cronin, *Appl. Phys. Lett.* **2007**, *91*, 223105.
[21] C. Oubre, P. Nordlander, *J. Phys. Chem. B* **2005**, *109*, 10042.
[22] P. Nordlander, C. Oubre, E. Prodan, K. Li, M. I. Stockman, *Nano Lett.* **2004**, *5*, 899.
[23] M. Alvaro, B. Cojocaru, A. A. Ismail, N. Petrea, B. Ferrer, F. A. Harraz, V. I. Parvulescu, H. Garcia, *Appl. Catal., B* **2010**, *99*, 191–197.
[24] K. Awazu, M. Fujimaki, C. Rockstuhl, J. Tominaga, H. Murakami, Y. Ohki, N. Yoshida, T. Watanabe, *J. Am. Chem. Soc.* **2008**, *130*, 1676–1680.
[25] M. Di Vece, A. B. Laursen, L. Bech, C. N. Maden, M. Duchamp, R. V. Mateiu, S. Dahl, I. Chorkendorff, *J. Photochem. Photobiol., A* **2012**, *230*, 10–14.
[26] P. Falaras, I. M. Arabatzis, T. Stergiopoulos, M. C. Bernard, *Int. J. Photoenergy* **2003**, *5*, 123–130.
[27] J. J. Feng, P. P. Zhang, A. J. Wang, Q. C. Liao, J. L. Xi, J. R. Chen, *New J. Chem.* **2012**, *36*, 148–154.
[28] D. M. Fouad, M. B. Mohamed, *J. Nanomater.* **2012**, *2012*, 1–8.
[29] J. Jiang, L. Z. Zhang, *Chem. Eur. J.* **2011**, *17*, 3710–3717.
[30] D. Kannaiyan, M. A. Cha, Y. H. Jang, B. H. Sohn, J. Huh, C. Park, D. H. Kim, *New J. Chem.* **2009**, *33*, 2431–2436.
[31] X. B. Ke, S. Ribbens, Y. Q. Fan, H. W. Liu, P. Cool, D. J. Yang, H. Y. Zhu, *J. Membr. Sci.* **2011**, *375*, 69–74.
[32] J. Y. Lan, X. M. Zhou, G. Liu, J. G. Yu, J. C. Zhang, L. J. Zhi, G. J. Nie, *Nanoscale* **2011**, *3*, 5161–5167.
[33] S. S. Malwadkar, R. S. Gholap, S. V. Awate, P. V. Korake, M. G. Chaskar, N. M. Gupta, *J. Photochem. Photobiol., A* **2009**, *203*, 24–31.
[34] I. Shown, M. Ujihara, T. Imae, *J. Nanosci. Nanotechnol.* **2011**, *11*, 3284–3290.
[35] H. Y. Song, Y. T. Yu, P. Norby, *J. Nanosci. Nanotechnol.* **2009**, *9*, 5891–5897.
[36] S. K. Tripathy, J. N. Jo, X. F. Wu, J. M. Yoon, Y. T. Yu, *J. Nanosci. Nanotechnol.* **2011**, *11*, 453–457.
[37] L. P. Wen, B. S. Liu, C. Liu, X. J. Zhao, *Journal of Wuhan University of Technology-Mater. Sci. Ed.* **2009**, *24*, 258–263.
[38] J. G. Yu, G. P. Dai, B. B. Huang, *J. Phys. Chem. C* **2009**, *113*, 16394–16401.

[39] I. M. Arabatzis, T. Stergiopoulos, D. Andreeva, S. Kitova, S. G. Neophytides, P. Falaras, *J. Catal.* **2003**, *220*, 127–135.
[40] C. Yogi, K. Kojima, T. Takai, N. Wada, *J. Mater. Sci.* **2009**, *44*, 821–827.
[41] C. Yogi, K. Kojima, N. Wada, H. Tokumoto, T. Takai, T. Mizoguchi, H. Tamiaki, *Thin Solid Films* **2008**, *516*, 5881–5884.
[42] X. Chen, H. Y. Zhu, J. C. Zhao, Z. T. Zheng, X. P. Gao, *Angew. Chem. Int. Ed.* **2008**, *47*, 5353–5356.
[43] J. F. Guo, B. W. Ma, A. Y. Yin, K. N. Fan, W. L. Dai, *Appl. Catal., B* **2011**, *101*, 580–586.
[44] W. B. Hou, Z. W. Liu, P. Pavaskar, W. H. Hung, S. B. Cronin, *J. Catal.* **2011**, *277*, 149–153.
[45] D. B. Ingram, P. Christopher, J. L. Bauer, S. Linic, *ACS Catal.* **2011**, *1*, 1441–1447.
[46] Z. X. Ji, M. N. Ismail, D. M. Callahan, E. Pandowo, Z. H. Cai, T. L. Goodrich, K. S. Ziemer, J. Warzywoda, A. Sacco, *Appl. Catal., B* **2011**, *102*, 323–333.
[47] S. T. Kochuveedu, D. P. Kim, D. H. Kim, *J. Phys. Chem. C* **2012**, *116*, 2500–2506.
[48] E. Kowalska, O. O. P. Mahaney, R. Abe, B. Ohtani, *Phys. Chem. Chem. Phys.* **2010**, *12*, 2344–2355.
[49] Y. Lu, H. T. Yu, S. Chen, X. Quan, H. M. Zhao, *Environ. Sci. Technol.* **2012**, *46*, 1724–1730.
[50] M. A. Mahmoud, W. Qian, M. A. El-Sayed, *Nano Lett.* **2011**, *11*, 3285–3289.
[51] M. M. Mohamed, K. S. Khairou, *Microporous Mesoporous Mater.* **2011**, *142*, 130–138.
[52] K. Mori, M. Kawashima, M. Che, H. Yamashita, *Angew. Chem. Int. Ed.* **2010**, *49*, 8598–8601.
[53] Y. Xie, J. Kum, X. J. Zhao, S. O. Cho, *Semicond. Sci. Technol.* **2011**, *26*, 1–6.
[54] J. B. Zhou, Y. Cheng, J. G. Yu, *J. Photochem. Photobiol., A* **2011**, *223*, 82–87.
[55] A. Primo, A. Corma, H. Garcia, *Phys. Chem. Chem. Phys.* **2011**, *13*, 886–910.
[56] D. S. Bhatkhande, V. G. Pangarkar, A. A. Beenackers, *J. Chem. Technol. Biotechnol.* **2001**, *77*, 102–116.
[57] A. Mills, R. H. Davies, D. Worsley, *Chem. Soc. Rev.* **1993**, *22*, 417–425.
[58] J. G. Yu, J. F. Xiong, B. Cheng, S. W. Liu, *Appl. Catal., B* **2005**, *60*, 211–221.
[59] H. X. Li, Z. F. Bian, J. Zhu, Y. N. Huo, H. Li, Y. F. Lu, *J. Am. Chem. Soc.* **2007**, *129*, 4538–4539.
[60] H. L. Duan, Y. M. Xuan, *Physica E: Low Dimens. Syst. Nanostruct.* **2011**, *43*, 1475–1480.
[61] Z. W. Liu, W. B. Hou, P. Pavaskar, M. Aykol, S. B. Cronin, *Nano Lett.* **2011**, *11*, 1111–1116.
[62] O. Rosseler, M. V. Shankar, M. K. L. Du, L. Schmidlin, N. Keller, V. Keller, *J. Catal.* **2010**, *269*, 179–190.
[63] C. G. Silva, R. Juarez, T. Marino, R. Molinari, H. Garcia, *J. Am. Chem. Soc.* **2011**, *133*, 595–602.
[64] T. Torimoto, H. Horibe, T. Kameyama, K. Okazaki, S. Ikeda, M. Matsumura, A. Ishikawa, H. Ishihara, *J. Phys. Chem. Lett.* **2011**, *2*, 2057–2062.
[65] D. B. Ingram, S. Linic, *J. Am. Chem. Soc.* **2011**, *133*, 5202–5205.
[66] W. B. Hou, W. H. Hung, P. Pavaskar, A. Goeppert, M. Aykol, S. B. Cronin, *ACS Catal.* **2011**, *1*, 929–936.
[67] X. J. Feng, J. D. Sloppy, T. J. LaTemp, M. Paulose, S. Komarneni, N. Z. Bao, C. A. Grimes, *J. Mater. Chem.* **2011**, *21*, 13429–13433.
[68] S. C. Roy, O. K. Varghese, M. Paulose, C. A. Grimes, *ACS Nano* **2010**, *4*, 1259–1278.
[69] O. K. Varghese, M. Paulose, T. J. LaTempa, C. A. Grimes, *Nano Lett.* **2009**, *9*, 731–737.
[70] K. Adachi, K. Ohta, T. Mizuno, *Sol. Energy* **1994**, *53*, 187–190.
[71] M. Halmann, V. Katzir, E. Borgarello, J. Kiwi, *Sol. Energy Mater.* **1984**, *10*, 85–91.
[72] M. Halmann, M. Ulman, B. Aurianblajeni, *Sol. Energy* **1983**, *31*, 429–431.
[73] T. Inoue, A. Fujishima, S. Konishi, K. Honda, *Nature* **1979**, *277*, 637–638.
[74] C. J. Wang, R. L. Thompson, J. Baltrus, C. Matranga, *J. Phys. Chem. Lett.* **2010**, *1*, 48–53.
[75] M. Anpo, H. Yamashita, Y. Ichihashi, S. Ehara, *J. Electroanal. Chem.* **1995**, *396*, 21–26.
[76] K. Koci, K. Mateju, L. Obalova, S. Krejcikova, Z. Lacny, D. Placha, L. Capek, A. Hospodkova, O. Solcova, *Appl. Catal., B* **2010**, *96*, 239–244.
[77] J. C. S. Wu, H. M. Lin, C. L. Lai, *Appl. Catal., A* **2005**, *296*, 194–200.
[78] J. C. S. Wu, T. H. Wu, T. C. Chu, H. J. Huang, D. P. Tsai, *Top. Catal.* **2008**, *47*, 131–136.
[79] E. B. Cole, P. S. Lakkaraju, D. M. Rampulla, A. J. Morris, E. Abelev, A. B. Bocarsly, *J. Am. Chem. Soc.* **2010**, *132*, 11539–11551.
[80] C.-C. Yang, Y.-H. Yu, B. van der Linden, J. C. S. Wu; G. Mul, *J. Am. Chem. Soc.* **2010**, *132*, 8398–8406.
[81] T. Yui, A. Kan, C. Saitoh, K. Koike, T. Ibusuki, O. Ishitani, *ACS Appl. Mater. Interfaces* **2011**, *3*, 2594–2600.
[82] K. Adachi, K. Ohta, T. Mizuno, *Sol. Energy* **1994**, *53*, 187–190.
[83] Y. Tian, T. Tatsuma, *Chem. Commun.* **2004**, *16*, 1810–1811.
[84] Y. Tian, T. Tatsuma, *J. Am. Chem. Soc.* **2005**, *127*, 7632–7637.
[85] B. O'Regan, M. Grätzel, *Nature* **1991**, *353*, 737.
[86] J. W. Tang, *ChemSusChem* **2010**, *3*, 800–801.
[87] W. T. Chen, Y. J. Hsu, P. V. Kamat, *J. Phys. Chem. Lett.* **2012**, *3*, 2493–2499.
[88] M. S. Devadas, K. Kwak, J.-W. Park, J.-H. Choi, C.-H. Jun, E. Sinn, G. Ramakrishna, D. Lee, *J. Phys. Chem. Lett.* **2010**, *1*, 1497–1503.
[89] I. Diez, R. H. A. Ras, *Nanoscale* **2011**, *3*, 1963–1970.
[90] C. M. Aikens, S. Li, G. C. Schatz, *J. Phys. Chem. C* **2008**, *112*, 11272–11279.
[91] J. Zheng, P. R. Nicovich, R. M. Dickson, *Annu. Rev. Phys. Chem.* **2007**, *58*, 409–431.
[92] A. Furube, L. Du, K. Hara, R. Katoh, M. Tachiya, *J. Am. Chem. Soc.* **2007**, *129*, 14852–14853.
[93] S. Mubeen, G. Hernandez-Sosa, D. Moses, J. Lee, M. Moskovits, *Nano Lett.* **2011**, *11*, 5548–5552.
[94] M. W. Knight, H. Sobhani, P. Nordlander, N. J. Halas, *Science* **2011**, *332*, 702–704.
[95] F. Le, D. W. Brandl, Y. A. Urzhumov, H. Wang, J. Kundu, N. J. Halas, J. Aizpurua, P. Nordlander, *ACS Nano* **2008**, *2*, 707–718.
[96] S. L. Zou, G. C. Schatz, *Chem. Phys. Lett.* **2005**, *403*, 62–67.
[97] V. Mizeikis, E. Kowalska, S. Juodkazis, *J. Nanosci. Nanotechnol.* **2011**, *11*, 2814–2822.
[98] S. Linic, P. Christopher, D. B. Ingram, *Nat. Mater.* **2011**, *10*, 911–921.
[99] K. Ueno, H. Misawa, *J. Photochem. Photobiol., A* **2011**, *221*, 130–137.
[100] H. Y. Zhu, X. B. Ke, X. Z. Yang, S. Sarina, H. W. Liu, *Angew. Chem. Int. Ed.* **2010**, *49*, 9657–9661.
[101] N. Chandrasekharan, P. V. Kamat, *J. Phys. Chem. B* **2000**, *104*, 10851–10857.
[102] P. V. Kamat, *J. Phys. Chem. C* **2007**, *111*, 2834–2860.
[103] K. Koci, K. Mateju, L. Obalova, S. Krejcikova, Z. Lacny, D. Placha, L. Capek, A. Hospodkova, O. Solcova, *Appl. Catal., B* **2010**, *96*, 239–244.
[104] A. Takai, P. V. Kamat, *ACS Nano* **2011**, *5*, 7369–7376.
[105] H. Choi, W. T. Chen, P. V. Kamat, *ACS Nano* **2012**, *6*, 4418–4427.
[106] A. Wood, M. Giersig, P. Mulvaney, *J. Phys. Chem. B* **2001**, *105*, 8810–8815.
[107] W. Y. Teoh, J. A. Scott, R. Amal, *J. Phys. Chem. Lett.* **2012**, *3*, 629–639.
[108] H. K. Mulmudi, N. Mathews, X. C. Dou, L. F. Xi, S. S. Pramana, Y. M. Lam, S. G. Mhaisalkar, *Electochem. Commun.* **2011**, *13*, 951–954.
[109] H. Dotan, K. Sivula, M. Gratzel, A. Rothschild, S. C. Warren, *Energy Environ. Sci.* **2011**, *4*, 958–964.